

# Multinuclear Solid-State MAS and CP-MAS NMR Study of the Binding of Triethyl Phosphate to a Montmorillonite

Paul O'Brien\* and Colin J. Williamson

Department of Chemistry, Queen Mary and Westfield College, University of London, Mile End Road, London, E1 4NS U.K.

Christopher J. Groombridge

Department of Chemistry, Royal Holloway and Bedford New College, Egham, Surrey, TW20 0EX, U.K.

Received July 25, 1990. Revised Manuscript Received October 24, 1990

The suitability of a clay for studies of the absorption/adsorption of organic molecules by multinuclear NMR spectroscopy can be judged from EPR spectra. The binding of triethyl phosphate to a montmorillonite, low in paramagnetic metal ions, has been studied by solid-state  $^{31}\text{P}$  and  $^{13}\text{C}$  NMR spectroscopy; magic angle spinning  $^1\text{H}$  NMR spectroscopy has been used to observe mobile phases within such solids. A number of mobile and immobile phases have been detected; one important mechanism in sorption probably involves coordination to the interlamellar cation. The results are discussed in terms of the utility of clays in a variety of applications.

## Introduction

Clay minerals, especially the smectite group, are widely used as absorbants/adsorbants in a range of applications including ion exchange, purification procedures, pharmaceuticals, and catalysis.<sup>1-4</sup> The interaction of ions (both organic and inorganic) and water with clays has been extensively studied, but the interaction of moderately polar organic molecules with smectite clays (especially in their normal hydrated state) is much less well understood.

The absorption of organic molecules must, in part, be due to the small particle size and wetting of the large external surface area of the clay. However, the most important factor in the absorption and retention of organic molecules by clays is their ability to swell and intercalate organic molecules within the interlamellar space.<sup>5</sup> The precise ways in which clays interact with organic molecules will be important in understanding the mobility of organic molecules, such as pesticides, in the geosphere, as well as traditional processes such as fulling and waste disposal.

Such interactions have been studied by a wide range of techniques, but x-ray diffraction<sup>2</sup> and infrared spectroscopy<sup>6</sup> are the most generally applied methods. NMR spectroscopy seems particularly appropriate for studying such systems and should provide information on structure and dynamics (local reorientation and diffusion) over a wide time scale, through a number of possible probe nuclei. In particular, observation of  $^{13}\text{C}$  spectra should be free of background from the clay matrix (in contrast to IR spectroscopy), and the use of solid-state NMR techniques<sup>7</sup> makes immobilized material observable. Resing et al.<sup>8</sup> have pointed out that clay minerals have sufficiently high surface area for  $^{13}\text{C}$  spectra to be obtained without isotopic

enrichment of the adsorbed species. However, the presence of trace levels of paramagnetic metal ions in natural clays leads to line broadening that severely limits the utility of the method (e.g., see ref 8) unless the clay sample is carefully chosen or is of synthetic origin.

Previously reported NMR studies have used systems such as benzene/hectorite,<sup>8</sup> 5'-AMP/bentonite,<sup>9</sup> 2-methylpropene/ hex-1-ene/Laponite (a synthetic hectorite),<sup>10,11</sup> and DMSO pyridine N-oxide/, formamide/, hydrazine/, and DMSeO/kaolinite.<sup>12,13</sup> The kaolinite intercalates were the only materials studied by the direct interaction of the clay with an organic liquid, rather than absorption of a vapor or from aqueous solution; however, kaolinites do not swell and are simpler because of the absence of interlayer cations and water. Furthermore, no previous study has followed the behavior of the absorbate as a function of relative proportions of organic and clay.

There are relatively few studies that address the speciation of organic molecules within the hydrated interlamellar space of smectite clays, and in this report we investigate the NMR spectroscopy of an organic molecule, triethyl phosphate (TEP), sorbed by a montmorillonite clay.

## Results and Discussion

**EPR Spectra and Initial Observations.** Fuller's earth, perhaps the most widely used form of montmorillonite, sorbs large quantities of organic molecules. However, a typical fuller's earth (such as Surrey Finest, Laporte Ind.) contains large quantities of paramagnetic impurities, especially iron and manganese; these can be seen in an EDAX<sup>14</sup> analysis of the clay. The metal ions also give rise to the characteristic ESR spectrum of the clay<sup>15</sup> as shown

(1) Adams, J. M.; Davies, S. E.; Graham, S. H.; Thomas, J. M. *J. Catal.* 1982, 78, 197.

(2) Barrer, R. M. *Philos. Trans. R. Soc. London, A* 1984, 311, 333.

(3) Odom, I. E. *Philos. Trans. R. Soc. London, A* 1984, 311, 391.

(4) Hall, P. L. *A Handbook of Determinative Methods in Clay Mineralogy*; Wilson, M. J., Ed.; Blackie: London, 1987; Chapter 1.

(5) Jones, T. R. *Clay Miner.* 1983, 18, 399.

(6) Bowen, J. M.; Powers, C. R.; Ratcliffe, A. E.; Rockley, M. G.; Hounslow, A. W. *Environ. Sci. Technol.* 1988, 22, 1178.

(7) Fyfe, C. A. *Solid State NMR for Chemists*; CRC Press: Boca Raton, FL, 1983.

(8) Resing, H. A.; Slotfeldt-Ellingsen, D.; Garraway, A. N.; Pinnavaia, T. J.; Unger, K. In *Magnetic Resonance in Colloid and Interface Science*; Fraissard, J. P., Resing, H. A., Eds.; 1980; p 239.

(9) Clayden, N. J.; Waugh, J. S. *J. Chem. Soc., Chem. Commun.* 1983, 292.

(10) Tennakoon, D. T. B.; Schlogl, R.; Rayment, T.; Klinowski, J.; Jones, W.; Thomas, J. M. *Clay Miner.* 1983, 18, 357.

(11) Tennakoon, D. T. B.; Thomas, J. M.; Jones, W.; Carpenter, T. A.; Ramdas, J. *J. Chem. Soc., Faraday Trans. 1* 1986, 82, 545.

(12) Thompson, J. G. *Clays Clay Miner.* 1985, 33, 173.

(13) Raupach, M.; Barron, P. F.; Thompson, J. G. *Clays Clay Miner.* 1987, 35, 208.

(14) Williamson, C. J., unpublished work.

(15) Craciun, C.; Meghea, A. *Clay Miner.* 1985, 20, 281.

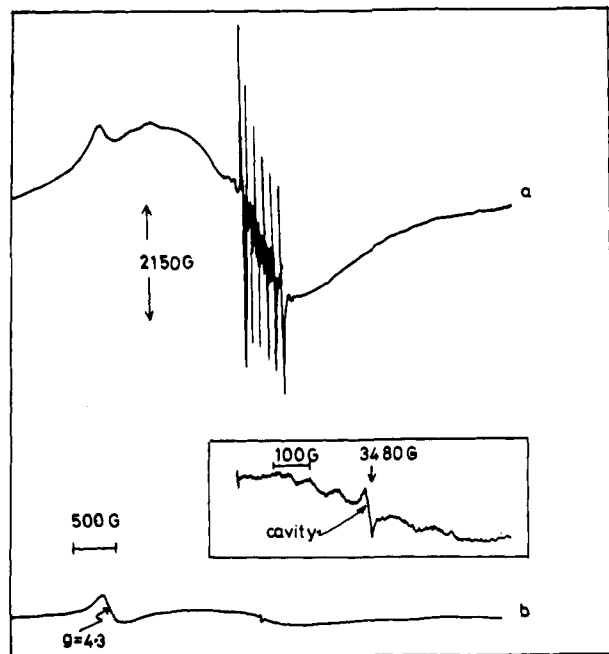


Figure 1. ESR spectra of clay samples, modulation amplitude 5, gain  $3.2 \times 10^4$ ; (a) fuller's earth; (b) westonite (inset at  $\times 10$  gain).

in Figure 1. The spectrum is dominated by a very broad feature ( $\sim 2500$  G) centred on  $g = 2.00$  due to coupled iron(III) centers. Six sharp lines due to manganese can also be observed (hyperfine splitting for Mn,  $I = 5/2$ ) superimposed on the broad absorption. There is also a half-field ( $g = 4.3$ ) line associated with isolated iron(III) centers. Attempts to obtain  $^{13}\text{C}$  solid-state NMR spectra for organic molecules adsorbed by fuller's earth samples were unsuccessful; a single very broad peak was observed, presumably because of relaxation effects associated with the paramagnetic ions. McWhinnie and co-workers have recently shown that magnetic susceptibility measurements are useful in determining the suitability of clay samples for solid-state NMR studies.<sup>16</sup>

We subsequently investigated a range of montmorillonites and found westonite (a magnesium montmorillonite obtained from English China Clays) to be low in paramagnetic metal ions; it hence seems to be an ideal model for fullers earth in NMR studies. EDAX measurements confirmed that iron and manganese were present at very low levels in this clay. The EPR spectrum is consequently weak compared to that of fuller's earth (Figure 1). Two main features can be seen, a half-field line at  $g = 4.3$  (isolated Fe(III) centers), and a weak absorption close to 3500 G. The latter is shown at higher gain, and although overlapping with a signal from the cavity this again appears to be a six-line spectrum characteristic of a trace of manganese.

**NMR Studies. Proton NMR spectra:** Despite the apparent dryness of all the TEP/clay mixtures, it is clear from  $^1\text{H}$  spectra that much of the added organic material exists as an essentially mobile liquid. Sharp resonances are observed in the  $^1\text{H}$  magic angle spinning (MAS) spectra (Figure 2); MAS at ca. 4.5 kHz would not be sufficient to give such narrow lines for a solid or restricted-motion phase. Sample spinning is useful, and for our samples essential, because its use reduces line broadening due to magnetic susceptibility effects in the heterogeneous systems. The starting hydrated montmorillonite shows a

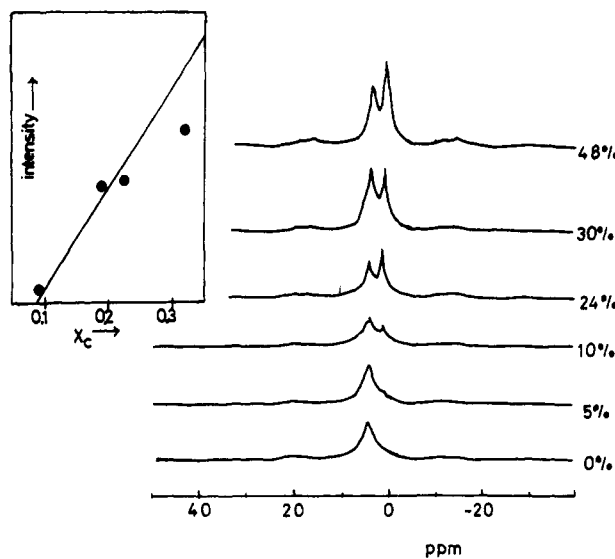


Figure 2.  $^1\text{H}$  magic angle spinning spectra. The inset shows a plot of the intensity of the methyl resonance as the doping is increased ( $X_c = W_{\text{TEP}}/(W_{\text{TEP}} + W_{\text{clay}})$ , the weight fraction of TEP on the clay). The data are scattered because spectra were run at different times; with variation in spectrometer performance the intercept is at about 10%.

broad Gaussian  $^1\text{H}$  line ( $\Delta\nu_{1/2} \sim 23$  kHz), a composite of hydroxyl protons in the aluminosilicate layer and bound interlamellar water, which is only partially narrowed by MAS, to  $\Delta\nu_{1/2} \sim 1200$  Hz. These results are comparable to those of Tennakoon,<sup>11</sup> who studied the synthetic montmorillonite Gelwhite.

The  $^1\text{H}$  line width of the liquid phase is probably dominated by magnetic susceptibility effects of the interspersed clay particles. These particles are expected to have small susceptibility anisotropy (especially if there is residual iron content), which gives a line broadening that is minimized but cannot be eliminated by MAS.<sup>17-19</sup> Thus the  $^1\text{H}$  MAS spectra show resolved methylene and methyl peaks in the expected 2:3 ratio but no  $J$  coupling fine structure (Figure 2,  $\delta(\text{CH}_2)$  1.35 ppm and  $\delta(\text{OCH}_2)$  4.14 ppm). The broad clay signal coincides with the TEP methylene peak, but the background can be subtracted from the liquid-phase TEP methyl signal, giving approximate liquid-phase quantitation.

**$^{31}\text{P}$  NMR spectra:** The  $^{31}\text{P}$  spectra provide clear evidence that, in addition to included liquid, some TEP is also tightly bound to the clay. NMR spectra do not change over considerable periods of time, indicating that TEP is stable within the clay matrix.

Spectra have been obtained in two ways:  $^{31}\text{P}$  90° single-pulse excitation and  $^{31}\text{P}^{\{1\text{H}\}}$  cross polarization (denoted by SPE-MAS and CP-MAS, respectively). Both experiments use high-power  $^1\text{H}$  decoupling, and SPE-MAS and CP-MAS regimes differ only in the manner of generation of  $^{31}\text{P}$  signal. The SPE-MAS spectrum should contain quantitative contributions from all phosphorus species, but it is possible that bound molecules have long  $T_1$ 's and are partially saturated at the chosen recycle time (usually 10 s).

The CP-MAS spectrum should consist only of immobilized species, since no CP signal is expected from liquids.

(17) Doskocilova, D.; Tao, D. D.; Schneider, B. *Czech. J. Phys. B* 1975, 25, 202.

(18) VanderHart, D. L.; Earl, W. L.; Garroway, A. N. *J. Magn. Reson.* 1981, 44, 361.

(19) Garroway, A. N. *J. Magn. Reson.* 1982, 49, 168.

(20) Rutar, V.; Kovac, M.; Lahajnar, J. *J. Magn. Reson.* 1988, 80, 133.

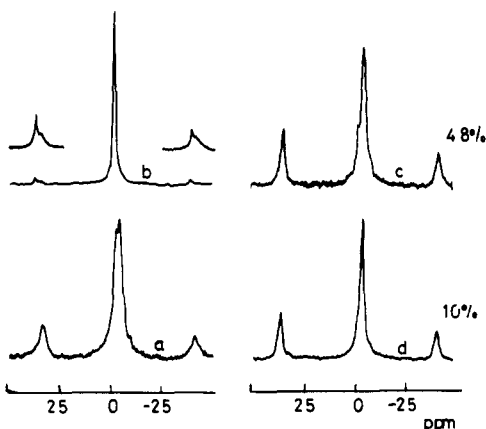


**Figure 3.**  $^{31}\text{P}$  spectra: (a) and (b) are SPE-MAS spectra; (c) and (d) are CP-MAS spectra; see also Table I.

**Table I.**  $^{31}\text{P}$  and  $^{13}\text{C}$  Solid-State NMR Results ( $\delta$  ppm)<sup>a</sup>

% w/w	$^{31}\text{P}$		$^{13}\text{C}$		
	MAS	CP-MAS	MAS	CP-MAS	contact time/ms
5			16.93, 65.33	17.05, 66.09	1.0
10	-2.76, -4.34	-3.77	17.14, 65.65	17.14, 66.59	1.0
24	-1.17	-3.66	16.67, 65.33	17.19, 65.63	1.0
30	-2.01	-4.78	16.63, 65.48	17.00, 65.65	1.0
48	-1.15	-3.93	16.66, 64.92	17.01, 66.66	0.2
55	-2.01	-4.90		17.00, 64.88	1.0
55				16.72, 64.92	6.0

<sup>a</sup> For the experimental conditions in typical experiments see the text.

CP can occur via  $J$  coupling for liquids, but the matching of the pulse amplitudes (the Hartmann-Hahn condition) is very much more stringent than for solids and is unlikely to be met.<sup>21</sup> Furthermore,  $J$ -CP is oscillatory and no such behavior is seen. Some direct  $^{31}\text{P}/^{13}\text{C}$  signal can be accidentally created, since the CP pulse can act as an excitation pulse for any initial  $^{31}\text{P}/^{13}\text{C}$  magnetization. However, this is largely suppressed by routinely using  $^1\text{H}$  spin-temperature inversion. Incomplete suppression may account for the weak shoulder at high loadings; otherwise the CP-MAS spectrum originates from the solid immobile domain only.

Figure 3 shows some typical  $^{31}\text{P}$  SPE and CP-MAS spectra. At low loadings (ca. 10%) the  $^{31}\text{P}$  SPE-MAS spectrum consists of two partially resolved peaks with nearly equal intensity. The peak can be deconvoluted into overlapping Lorentzian peaks centered at -2.8 and -4.3 ppm (Figure 3a, Table I), and approximately equal intensity. The observed intensity did not vary for recycle delays of 5 and 10 s, so both of the  $^{31}\text{P}$  species are fully relaxed (i.e.,  $T_1$  less than 1 s) and the intensity reflects true relative quantities (Figure 4).

As the TEP content is increased, the high-frequency component increases roughly linearly, while the low-frequency feature remains nearly constant and, at very high TEP level, is observable only as a slight peak asymmetry.

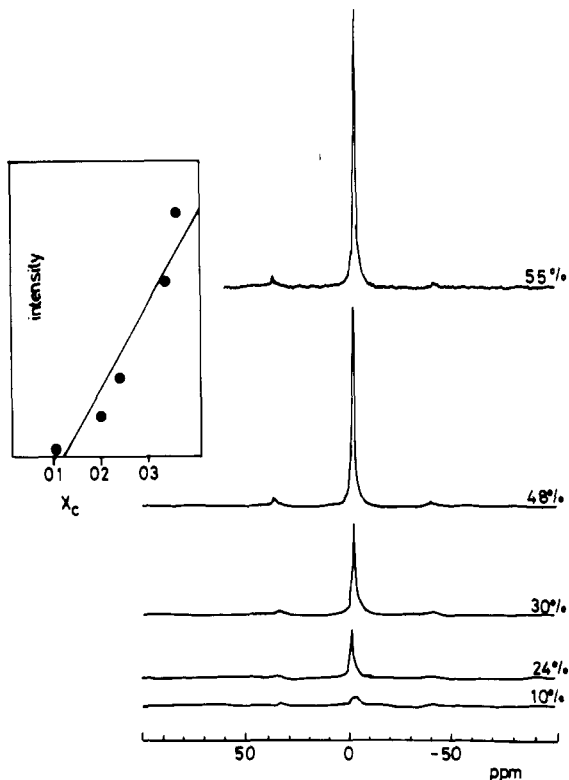


**Figure 4.**  $^{31}\text{P}$  SPE spectra at increased doping. The inset shows a plot of the intensity of the  $^{31}\text{P}$  resonance as the doping is increased ( $X_c$  is defined in the caption to Figure 2). The data are scattered because spectra were run at different times, with variation in spectrometer performance.

(Figure 3b). However, the spinning sidebands of the -2.8 ppm peak are weak compared to those for the -4.3 ppm resonance.

The use of cross polarization demonstrates that the low-frequency peak comes from a bound site: the CP-MAS spectra contain only this resonance and are largely constant at all loadings (Figure 3c,d and Table I). The CP-MAS spectra also show more clearly than the  $^{31}\text{P}$  chemical shift has a small anisotropy (probably motionally averaged). Analysis of the spinning sideband intensities gives chemical shift tensor principal components of -63, +2, and +50 ppm ( $\pm 10$  ppm). These results are similar to those obtained by Clayden and Waugh<sup>9</sup> for 5-AMP absorbed on zinc-exchanged bentonite. A chelating phosphate might be expected to present a more symmetrical environment ( $\sigma_{11} = \sigma_{22}$ ); consequently, we suggest in the present case that the TEP molecule is coordinated through one oxygen to the interlamellar cation, magnesium.

**$^{13}\text{C}$  NMR spectra:** The  $^{13}\text{C}$  spectra support the  $^1\text{H}$  and  $^{31}\text{P}$  evidence but reveal a more complicated situation for the immobilized material. The SPE-MAS spectra show the expected two peaks: methylene at ca 65 ppm and methyl at ca 17 ppm (Figure 5, Table I), which grow in intensity as the trapped liquid phase increases. A broad background signal is also seen and is known to come from fluorocarbon polymers in the MAS probehead (Kel-F rotor endcap, Teflon cable dielectrics). Since these materials contain no protons, this signal is absent in CP-MAS spectra.

At all TEP levels some organic material is sufficiently immobilized in a solidlike environment for cross polarization to become possible, as shown by the series of  $^{13}\text{C}$  CP-MAS spectra (Figure 5). Both methylene and methyl resonances are shifted relative to the liquid-phase material, which dominates the SPE-MAS spectra, and the methy-

(21) Bertrand, R. D.; Moniz, W. B.; Garroway, A. N.; Chingao, G. C. *J. Am. Chem. Soc.* 1978, 100, 5227.

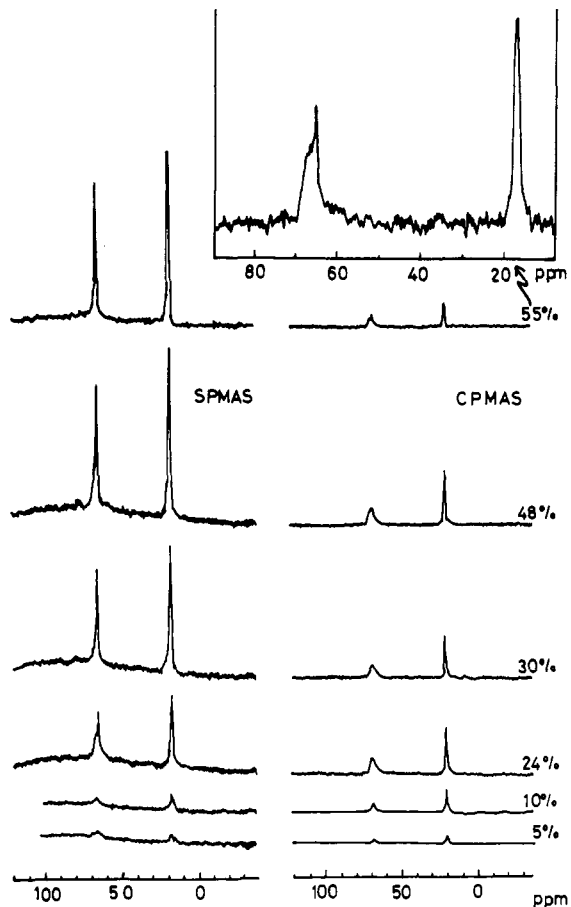


Figure 5.  $^{13}\text{C}$  spectra SPE + CP-MAS at various dopings. The inset shows an expansion emphasising the asymmetry of the methylene resonance.

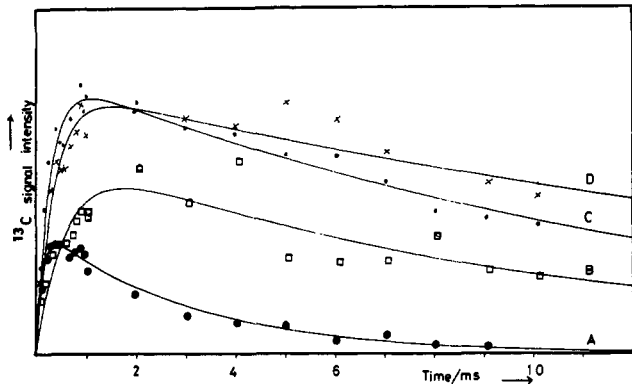


Figure 6.  $^{13}\text{C}$  Cross-polarization behavior of a sample of TEP (55%) on westonite: (A) methylene, 67.0 ppm; (B) methylene, 65 ppm; (C) methyl, 17.0 ppm; (D) methyl, 16.7 ppm.

lene resonance is clearly a composite of at least two overlapping lines. A reasonable fit is obtained by using two Lorentzian lineshapes (Figure 5, inset; parameters, chemical shifts 66.1 and 64.9 ppm, line widths 327 and 50 Hz). The methyl peak must also consist of at least two lines that are near degenerate.

This is more clearly defined by a series of spectra in which the CP contact time has been varied (Figure 6) to examine the  $^{13}\text{C}$ - $^1\text{H}$  cross-relaxation dynamics. This experiment is most useful but requires extensive spectrometer time and is not practicable for every sample. A reasonable compromise for this sort of system is the acquisition of CP-MAS spectra at two or three contact times (0.4, 1, 4 ms). Some typical results are shown in Table I.

Table II. Cross Relaxation Behavior of  $^{13}\text{C}$  Resonances (55% w/w)

resonance	$\delta/\text{ppm}$	$T_{\text{CH}}/\mu\text{s}$	$T_{1\rho}/\text{ms}$
$\text{CH}_3$	16.7	366	21.3
$\text{CH}_3$	17.0	280	13.4
$\text{CH}_2$	65.0	572	10.7
$\text{CH}_2$	67.0	121	3.0

Figure 6 shows the experimental data for the intensity of magnetization at four positions in the spectrum as a function of contact time. The data are somewhat scattered but can be fitted to the well-documented theoretical equations,<sup>22</sup> and three parameters extracted:  $I_{\infty}$ ,  $T_{\text{CH}}$ , and the sum  $T_{1\rho\text{H}} + T_{1\rho\text{C}}$ . The strength of  $^1\text{H}$ - $^1\text{H}$  dipolar coupling leads to a common value of  $T_{1\rho\text{H}}$  for all protons in a domain of a sample, whereas  $I_{\infty}$ ,  $T_{\text{CH}}$ , and  $T_{1\rho\text{C}}$  are specific to individual carbons. The two methylene absorptions are reasonably well separated at the selected frequencies, so the cross-relaxation curves (Figure 6A,B) represent the unmixed behavior of the two  $^{13}\text{C}$  atoms/sites. This behavior is quite different, in respect of the rotating frame relaxation (see fitted parameters in Table II).

The results for the two frequencies within the methyl band are more ambiguous because although it seems likely that similar short-plus-long  $T_{1\rho}$  curves are present, these are almost completely superimposed. The intensity-weighted center shifts slightly as the relative contributions change, from which the concealed shift splitting can be estimated as 0.2 ppm.

$^{13}\text{C}$  relaxation is often less efficient than that of protons or  $^{31}\text{P}$  because homonuclear couplings are larger than the  $^{13}\text{C}$ - $^1\text{H}$  couplings, in part a consequence of the larger magnetogyric ratio, so it is common to assume that  $T_{1\rho\text{C}}$  is much longer than  $T_{1\rho\text{H}}$ . If there were so, the different methylene peak  $T_{1\rho}$  decay behavior would imply discrete domains for these two species. However, it is also possible that a bound TEP molecule undergoes restricted motion at a frequency that makes  $T_{1\rho\text{C}}$  particularly short.<sup>23</sup>

### Conclusions

The results of this study clearly indicate that there are a number of different environments for TEP within the clay. These include a mobile phase and at least two motion-restricted species.

The organic material is mostly held as trapped liquid, but there is some evidence of a change of liquid properties as indicated by the line widths—due to mixing with water or viscosity change as suggested from MAS studies ( $^1\text{H}$ ,  $^{13}\text{C}$ , and  $^{31}\text{P}$ ). Some of the mobile material may be on the surface of the clay, but some is probably within the interlamellar space. The “liquid phase” line widths were found to be roughly equal (in ppm) for  $^1\text{H}$ ,  $^{13}\text{C}$ , and  $^{31}\text{P}$  and thus are probably governed by susceptibility effects of the kind described by Doskoscilova et al.<sup>17</sup>

Mobile TEP is present in all samples and may indicate either that the systems have not fully equilibrated or that the mobile phase is in equilibrium with the immobilized species even at low percentages of doping. MAS spectra were reproducible over a period of time, so either the system reaches equilibrium very slowly or there is an equilibrium amount of the mobile phase. In either case the presence of mobile phases has implications for the use

(22) Mehring, M. *Principles of High Resolution NMR in Solids*, 2nd ed.; Springer-Verlag: Berlin, 1983.

(23) Garroway, A. N. *J. Magn. Reson.* 1979, 34, 283.

of such clays in sustained release and waste control applications.

There are at least two sites for bound TEP, which could be explained as either internal and external TEP, or perhaps more probably interlamellar TEP in two distinct environments bound to the magnesium.

However, in each case TEP is bound through one oxygen, probably to a cation.<sup>10</sup> The quantity of bound material can be estimated as about 10% w/w (100 mg/g). The achievable detection limit depends very much on line width, and paramagnetic-free clays (synthetic) would be useful for such work. However, our study serves to show that a great deal of information concerning the nature of organic molecules absorbed and adsorbed by clays can be obtained by solid-state NMR methods.

### Experimental Section

**Materials.** Surrey Finest (fuller's earth) was characterized by a water content of 12% w/w (by TGA) and a *d*(001) spacing of 14.7 Å, characteristic of two layers of intercalated water.<sup>4</sup> Westomite was characterized by a water content of 13% w/w (by TGA) and a *d*(001) spacing of 14.7 Å, characteristic of two layers of intercalated water. Samples were prepared by grinding TEP with the solid clay until the sample appeared homogeneous. Triethyl phosphate was purchased from British Drug Houses, dried over molecular sieves, and distilled before use. Purity was confirmed by high-resolution solution <sup>13</sup>C and <sup>31</sup>P NMR spectroscopies.

**Instrumentation.** ESR spectra were recorded with a Bruker ERD 2000/10 at room temperature; water content was estimated by thermogravimetry with a Stanton Redcroft TG-750 TGA.

NMR spectra were recorded with a Bruker MSL-300 instrument with <sup>1</sup>H, <sup>13</sup>C, and <sup>31</sup>P frequencies of 300.13, 75.47, and 121.49 MHz, respectively. No line broadening was applied to any spectra. <sup>1</sup>H and <sup>13</sup>C shifts are in ppm relative to liquid TMS, <sup>31</sup>P are measured in ppm relative to 85% phosphoric acid by replacement.

<sup>13</sup>C spectra were referenced by replacement to the methylene peak of solid adamantane, to give a scale equivalent to TMS.<sup>24</sup>

The probe dead time for <sup>1</sup>H MAS spectra was approximately 6 ms, so broad features (>30 kHz) will be distorted or attenuated. <sup>31</sup>P spectra were recorded in MAS experiments typically: 2000 scans, a 10 s delay, 4-ms acquisition time. CP-MAS experiments were typically: 10 000 scans, a 5-s delay, an acquisition time of 16 ms, and a contact time of 1 ms. In both cases the sweep width was 125 kHz with 70-kHz proton decoupling. <sup>13</sup>C spectra were recorded in single-pulse magic angle spinning experiments, with typical conditions: 400 scans, a 10-s recycle delay, and 34-ms acquisition time. Cross-polarization magic angle spinning experiments (CP-MAS) were typically: 2000 scans, a 2-s delay, an acquisition time of 34 ms, and a contact time of 1 ms. In both cases the sweep width was 30 kHz with 70-kHz proton decoupling.

The <sup>13</sup>C Hartmann-Hahn condition was set by using slowly spinning adamantane (ca. 1.5 kHz). The match position for this is sensitive to changes of ca. 5% in either the <sup>1</sup>H or <sup>13</sup>C radio frequency field. The <sup>31</sup>P match was found by using slowly spinning NH<sub>4</sub>H<sub>2</sub>PO<sub>4</sub>. The signal strength is less sensitive to mismatch than adamantane/<sup>13</sup>C, but the <sup>1</sup>H and <sup>31</sup>P fields are likely to be equal within 20%.

Experiments to assess the quantities of bound material were carried out at different times during the study and are at best semiquantitative. The absolute intensity mode was used, with due allowance for differences in the number of scans; arbitrary intensity is plotted in terms of the peak area (see Figures 1 and 4).

**Acknowledgment.** This work was supported by the Procurement Executive of the Ministry of Defence. Spectra were recorded by the ULIRS solid-state NMR service of the University of London: the sample of westomite was a gift from English China Clays.

**Registry No.** TEP, 78-40-0; montmorillonite, 1318-93-0.

(24) Earl, W. L.; VanderHart, D. L. *J. Magn. Reson.* 1982, 48, 35.

## Vaporization Processes of Aluminum $\beta$ -Diketone Chelates

Y. Pauleau\* and O. Dulac

*Institut National Polytechnique de Grenoble, ENSEEG, B.P. 75, 38402, Saint Martin d'Hères, France*

Received August 3, 1990. Revised Manuscript Received December 12, 1990

Aluminum(III) trifluoro- and hexafluoroacetylacetones, Al(C<sub>5</sub>H<sub>4</sub>F<sub>3</sub>O<sub>2</sub>)<sub>3</sub> and Al(C<sub>5</sub>HF<sub>6</sub>O<sub>2</sub>)<sub>3</sub>, were prepared by reaction of aluminum isopropoxide with the corresponding fluorinated acetylacetone in benzene solution. The kinetics of vaporization of these fluorinated aluminum complexes and aluminum(III) acetylacetone, Al(C<sub>5</sub>H<sub>7</sub>O<sub>2</sub>)<sub>3</sub>, was investigated by isothermal thermogravimetry at temperatures ranging from 70 to 190 °C with an hydrogen or argon pressure varying between 100 and 300 Torr. The vaporization process was found to be rate-limited by the diffusion of these large complex molecules in the buffer gas (H<sub>2</sub> or Ar). The activation energy of these processes was demonstrated to be equal to the standard enthalpy of sublimation or evaporation of metal complexes. The values of the standard enthalpy of sublimation or evaporation of aluminum(III) complexes were compared with those reported in the literature and determined by other techniques. A comparison of the volatility of these metal complexes in terms of mass of aluminum evolved in the gas phase per minute as a function of vaporization temperature is also presented in this paper and can serve as a guideline for the selection of a suitable precursor in chemical vapor deposition of aluminum-containing films.

### Introduction

Metal complexes and organometallic compounds such as metal alkyls, metal alkoxides,  $\beta$ -diketonates, and cyclopentadienyl derivatives are under intensive investigation since these compounds are attractive candidates to be used as volatile precursors in chemical vapor deposition (CVD) of ceramic materials, new superconductors, and other

various insulating or conductive thin films.<sup>1-5</sup> Aluminum acetylacetone, Al(C<sub>5</sub>H<sub>7</sub>O<sub>2</sub>)<sub>3</sub> or Al(acac)<sub>3</sub>, appears as an

(1) Suhr, H.; Bald, J.; Deutschmann, L.; Etspueler, A.; Feurer, E.; Grunwald, H.; Haag, C.; Holzschuh, H.; Oehr, Reich, S.; Schmid, R.; Traus, I.; Wainer, B.; Weber, A.; Wendel, H. *J. Phys. (Paris)* 1989, 50, C5, 739.

(2) Schleich, D. M. *J. Phys. (Paris)* 1989, 50, C5 (supplement), 961.